

# Inverse design of cooperative electromagnetic interactions

M. Langlais,<sup>1,2</sup> J. P. Hugonin,<sup>1</sup> M. Besbes,<sup>1</sup> and P. Ben-Abdallah<sup>1,\*</sup>

<sup>1</sup>*Laboratoire Charles Fabry, UMR 8501, Institut d'Optique, CNRS, Université Paris-Sud 11, 2, Avenue Augustin Fresnel, 91127 Palaiseau Cedex, France.*

<sup>2</sup>*Total New Energies, R&D, Tour Michelet, 92078 Paris La Défense Cedex, France.*

(Dated: February 28, 2024)

The cooperative electromagnetic interactions between discrete resonators have been widely used to modify the optical properties of metamaterials. Here we propose a general evolutionary approach for engineering these interactions in arbitrary networks of resonators. To illustrate the performances of this approach, we designed by genetic algorithm, an almost perfect broadband absorber in the visible range made with a simple binary array of metallic nanoparticles.

PACS numbers: 42.25.Fx, 42.50.Nn, 84.60.-h, 02.60.Pn, 78.67.-n, 42.25.Bs

Engineering light-matter interactions is a longstanding problem in physics and is of prime importance for numerous technological applications such as the photo and thermophovoltaic energy conversion [1, 2], the optical manipulation of nanoobjects [3] or the quantum information treatment [4]. Light interaction with resonant structures embedded inside a material is a natural way to modify its optical properties. To date, a large number of resonant structures have been developed following such a strategy. Among these, metamaterials based on metallo-dielectric structures have been proposed to operate at frequencies ranging from the microwave domain [5] to the visible [6].

The design of artificially constructed magnetodielectric resonators which strongly interact cooperatively is a very recent and promising way to generate metamaterials that highlight innovative physical [7, 8] and transport [9] properties. However, so far, only heuristic approaches have been followed to identify the convenient meta-structures which display target functionalities. In the present Letter, we present a general theory to describe the multiple scattering interactions mechanisms in discrete networks of resonators embedded in a host material and we propose an evolutionary method to identify the appropriate inner structure of networks that highlight a targeted optical property. To illustrate the strong potential of cooperative interactions to tailor the optical properties of materials we design, by using a genetic algorithm, a broadband light absorber made with simple binary lattices of metallic nanoparticles immersed in a transparent host material.

To start, let us consider a set of objects dispersed inside a host material as depicted in Fig. 1. Suppose this system is highlighted by an external harmonic electromagnetic field of wavelength much larger than the typical size of objects. In this condition, we can associate to each object an electric (E) and magnetic (H) dipole moment  $\mathbf{p}_{i,A}$  ( $A = E, H$ ) (the higher orders contributions are discussed in the supplemental material [10]). The local electromagnetic field  $\mathbf{A}^{ext}(\mathbf{r}_i)$  at the dipoles location  $\mathbf{r}_i$  results from the superposition of external inci-

dent field, the field generated by the others dipoles and the auto-induced field which comes from the interactions with the interfaces. Therefore it takes the form

$$\mathbf{A}_i^{ext} = \mathbf{A}_i^{inc} - i\omega \sum_{B=E,H} \Gamma_{AB} \left( \sum_{j \neq i} \mathbb{G}_{ij}^{AB} \mathbf{p}_{j,B} + \Delta \mathbb{G}_{ii}^{AB} \mathbf{p}_{i,B} \right), \quad (1)$$

where  $\begin{pmatrix} \Gamma_{EE} & \Gamma_{EH} \\ \Gamma_{HE} & \Gamma_{HH} \end{pmatrix} \equiv \begin{pmatrix} i\omega\mu_0 & \omega/c \\ \omega/c & -i\omega\epsilon_0 \end{pmatrix}$  and  $\mathbb{G}_{ij}^{AB}$  is the dyadic Green tensor in the host material which takes into account the presence of interfaces and gives the field  $\mathbf{A}$  at the position  $\mathbf{r}_i$  given a  $\mathbf{B}$ -dipole located in  $\mathbf{r}_j$ .  $\Delta \mathbb{G}^{AB}$  defined as  $\Delta \mathbb{G}^{AB} \equiv \mathbb{G}^{AB} - \mathbb{G}_0^{AB}$  gives the contribution of interfaces only. Here  $\mathbb{G}_0^{AB}(\mathbf{r}_i, \mathbf{r}_j) = \frac{\exp(ikr_{ij})}{4\pi r_{ij}} \times$

$\begin{cases} \left[ \left( 1 + \frac{ikr_{ij}-1}{k^2 r_{ij}^2} \right) \mathbb{1} + \frac{3-3ikr_{ij}-k^2 r_{ij}^2}{k^2 r_{ij}^2} \hat{\mathbf{r}}_{ij} \otimes \hat{\mathbf{r}}_{ij} \right] & \text{if } A = B \\ \frac{ikr_{ij}-1}{kr_{ij}} \mathbb{L} & \text{if } A \neq B \end{cases}$  is the free space Green tensor in the host material defined with the unit vector  $\hat{\mathbf{r}}_{ij} \equiv \mathbf{r}_{ij}/r_{ij}$ .  $\mathbf{r}_{ij}$  denotes here the vector linking the center of dipoles  $i$  and  $j$ , while  $r_{ij} = |\mathbf{r}_{ij}|$ ,  $k$  is the wavevector,  $\mathbb{1}$  the unit dyadic tensor and  $\mathbb{L} = \begin{pmatrix} 0 & -\hat{r}_{ij,z} & \hat{r}_{ij,y} \\ \hat{r}_{ij,z} & 0 & -\hat{r}_{ij,x} \\ -\hat{r}_{ij,y} & \hat{r}_{ij,x} & 0 \end{pmatrix}$ . Beside the dipoles location the auto-induced part of field does not exist anymore and it takes the simplified form

$$\mathbf{A}^{ext}(\mathbf{r}) = \mathbf{A}^{inc}(\mathbf{r}) - i\omega \sum_{B=E,H} \Gamma_{AB} \sum_j \mathbb{G}^{AB}(\mathbf{r} - \mathbf{r}_j) \mathbf{p}_{j,B}. \quad (2)$$

It immediately follows that, the dipolar moments associated to each object reads

$$\mathbf{p}_{i,A} = \chi_A \overleftrightarrow{\alpha}_{i,A} \mathbf{A}_i^{ext} \quad (3)$$

where  $\chi_A$  represents either the vacuum permittivity  $\epsilon_0$  or the vacuum permeability  $\mu_0$  and  $\overleftrightarrow{\alpha}_{i,A}$  is the free polarizability tensor of  $i^{th}$  object under the action of field  $\mathbf{A}$ . By inserting the external contribution (1) of local field into relation (3) we get the following system which

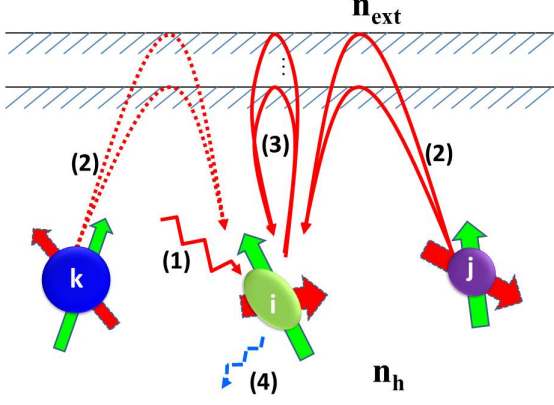


Figure 1: Multiple light scattering interactions in a set of subwavelength plasmonic structures embedded in a transparent host material of refractive index  $n_h$ . In the dipolar approximation each object is replaced by both a dipolar electric moment and a magnetic moment. The external field felt by each object decomposes into (1) the incident field, (2) the field radiated by the other objects and (3) the auto-induced field which comes from the interface after being emitted by the object itself. All dipoles radiate (4) in their surrounding.

relates all dipole moments

$$\mathbf{p}_{i;A} = \chi_A \overleftrightarrow{\alpha}_{i;A} [\mathbf{A}_i^{inc} - i\omega \sum_j \sum_{B=E,H} \mathbf{G}_{reg}^{AB}(r_i, r_j) \mathbf{p}_{j;B}]. \quad (4)$$

Here, where we have introduced the regularized Green tensor

$$\mathbf{G}_{reg}^{AB}(r, r') = \begin{cases} \Gamma_{AB} \mathbf{G}^{AB}(r, r') & \text{if } r \neq r' \\ \Gamma_{AB} \Delta \mathbf{G}^{AB}(r, r') & \text{if } r = r' \end{cases}. \quad (5)$$

In the particular case of  $n$ -ary periodic lattices made with  $n$  arbitrary dipoles of free electric or magnetic polarizability  $\overleftrightarrow{\alpha}_{i;A=E,H}$  distributed in a unit cell we have, according to the periodicity, the supplementary relations for the incident fields  $\mathbf{A}_{j\beta}^{inc} = \mathbf{A}_\beta \exp(i\mathbf{k}_{//} \cdot \mathbf{r}_{j\beta})$  and for the dipolar moments  $\mathbf{p}_{j\beta;A} = \tilde{\mathbf{p}}_{\beta;A} \exp(i\mathbf{k}_{//} \cdot \mathbf{r}_{j\beta})$ . Here  $\mathbf{r}_{j\beta}$  is the position vector of the  $\beta^{th}$  dipole inside the unit cell  $j$  of lattice and  $\mathbf{k}_{//}$  is the parallel component of wavevector. Accordingly, Eq. (4) can be solve with respect to the incident field to give

$$\begin{pmatrix} \tilde{\mathbf{p}}_E \\ \tilde{\mathbf{p}}_H \end{pmatrix} = \mathcal{A}^{-1} \mathcal{H} \begin{pmatrix} \tilde{\mathbf{E}} \\ \tilde{\mathbf{H}} \end{pmatrix}. \quad (6)$$

Here we have set  $\tilde{\mathbf{p}}_{A=E,H} = (\tilde{\mathbf{p}}_{1,A}, \dots, \tilde{\mathbf{p}}_{n,A})^t$  and  $\tilde{\mathbf{A}} = (\tilde{\mathbf{A}}_1, \dots, \tilde{\mathbf{A}}_n)^t$  and we have define the block matrixes

$$\mathcal{H} = \text{diag}(\varepsilon_0 \overleftrightarrow{\alpha}_{1;E}, \dots, \varepsilon_0 \overleftrightarrow{\alpha}_{n;E}, \mu_0 \overleftrightarrow{\alpha}_{1;H}, \dots, \mu_0 \overleftrightarrow{\alpha}_{n;H}) \quad (7)$$

and

$$\mathcal{A} = \begin{pmatrix} (1 + \mathbf{U}_{11}^{EE}) & \mathbf{U}_{12}^{EE} & \dots & \mathbf{U}_{1n}^{EE} & \mathbf{U}_{11}^{EH} & \dots & \mathbf{U}_{1n}^{EH} \\ \mathbf{U}_{21}^{EE} & \ddots & & \vdots & \vdots & & \vdots \\ \vdots & \ddots & (1 + \mathbf{U}_{nn}^{EE}) & \mathbf{U}_{n-1,n}^{EE} & \mathbf{U}_{n1}^{EH} & \dots & \mathbf{U}_{nn}^{EH} \\ \mathbf{U}_{n1}^{EE} & \dots & \mathbf{U}_{n,n-1}^{EE} & (1 + \mathbf{V}_{11}^{HH}) & \mathbf{V}_{12}^{HH} & \dots & \mathbf{V}_{1n}^{HH} \\ \mathbf{V}_{11}^{HE} & \dots & \mathbf{V}_{1n}^{HE} & \mathbf{V}_{21}^{HH} & \ddots & \ddots & \vdots \\ \vdots & & \vdots & \vdots & \ddots & \ddots & \mathbf{V}_{n-1,n}^{HH} \\ \mathbf{V}_{n1}^{HE} & \dots & \mathbf{V}_{nn}^{HE} & \mathbf{V}_{n1}^{HH} & \dots & \mathbf{V}_{n,n-1}^{HH} & (1 + \mathbf{V}_{nn}^{HH}) \end{pmatrix} \quad (8)$$

with

$$\mathbf{U}_{lk}^{EA} = i\varepsilon_0 \omega \overleftrightarrow{\alpha}_{l;E} \sum_j \mathbf{G}_{reg}^{EA}(\mathbf{r}_{0l}, \mathbf{r}_{jk}) e^{i\mathbf{k}_{//} \cdot (\mathbf{r}_{jk} - \mathbf{r}_{0l})}, \quad (9)$$

$$\mathbf{V}_{lk}^{HA} = i\mu_0 \omega \overleftrightarrow{\alpha}_{l;H} \sum_j \mathbf{G}_{reg}^{HA}(\mathbf{r}_{0l}, \mathbf{r}_{jk}) e^{i\mathbf{k}_{//} \cdot (\mathbf{r}_{jk} - \mathbf{r}_{0l})}. \quad (10)$$

Relation (6) defines the dressed polarizability tensor

$$\mathbf{\Upsilon} \equiv \mathcal{A}^{-1} \mathcal{H} = \begin{pmatrix} \mathbf{\Upsilon}^{EE} & \mathbf{\Upsilon}^{EH} \\ \mathbf{\Upsilon}^{HE} & \mathbf{\Upsilon}^{HH} \end{pmatrix} \quad (11)$$

of resonators within the unit cell of lattice. We clearly see that this polarizability is resonant when  $\det \mathcal{A} = 0$ . The former condition depends only on the intrinsic properties of materials while the second is of geometric nature and depends on the spatial distribution of nanostructures [11].

The power dissipated inside each resonator at a frequency  $\omega$  is given by the rate of doing work by the fields

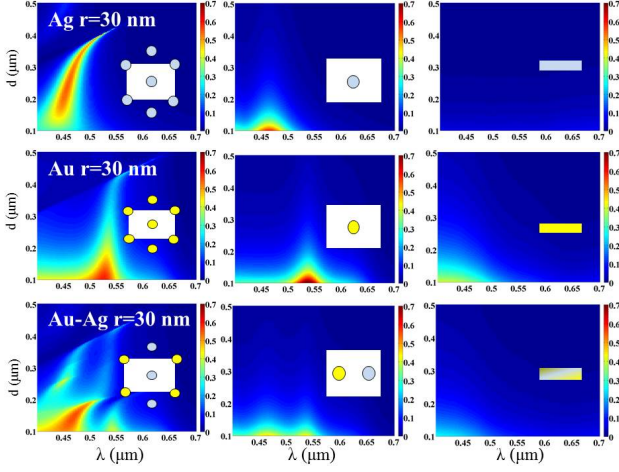


Figure 2: On the first column, absorption of simple and binary hexagonal lattices made with Ag and Au nanoparticles 30 nm radius immersed at  $h = 100\text{nm}$  from the surface in a transparent host medium of index  $n_h = 1.5$  with respect to the density in particles. On the second column, this absorption is compared with the absorption of single particles without multiple scattering interaction and, on the last column, with the results given by the effective medium theory with the same filling factor.

in its volume  $V_i$

$$\mathcal{P}_i(\omega) = \frac{1}{2} \sum_{A=E,H} \int_{V_i} \text{Re}[\mathbf{j}_A^*(\mathbf{r}, \omega) \cdot \mathbf{A}(\mathbf{r}, \omega)] d\mathbf{r}. \quad (12)$$

Here  $\mathbf{A}$  denotes either the local electric or magnetic field  $\mathbf{E}$  and  $\mathbf{H}$  while  $\mathbf{j}_E$  and  $\mathbf{j}_H$  are the corresponding local current density. In the dipolar approximation  $\mathbf{j}_{i;A} = -i\omega \mathbf{p}_{i;A} \delta(\mathbf{r} - \mathbf{r}_i)$ , expression (12) can be recasted into the discrete form

$$\begin{aligned} \mathcal{P}_i(\omega) = & -\frac{\omega}{2} \sum_{A=E,H} \{ \text{Im}[\mathbf{p}_{i;A}^*(\omega) \cdot \mathbf{A}_i^{ext}(\omega)] \\ & - \frac{\omega^3 \mu_0}{2} \mathbf{p}_{i;A}^* \text{Im}[\mathbf{G}_0^{AA}(\mathbf{r}_i, \mathbf{r}_i)] \mathbf{p}_{i;A} \}. \end{aligned} \quad (13)$$

By inverting (1) after having replaced the dipole moments by their expression with respect to  $\mathbf{A}_i^{ext}$ , we can express  $\mathbf{A}_i^{ext}$  in term of  $\mathbf{A}_{inc}$  and explicitly calculate the power dissipated in each object under an external lighting.

For spherical particles of radius  $R$  the polarizability is straightforwardly derived from the Mie scattering theory [12]. If those particles, of refractive index  $n_m$ , are immersed inside a medium of index  $n_h$ , we have  $\overleftrightarrow{\alpha}_A = \alpha_A \mathbb{1}$  with

$$\alpha_E^{-1} = k_0^3 \frac{n_h}{6\pi} (C_E - i), \quad (14)$$

$$\alpha_H^{-1} = k_0^3 \frac{n_h}{6\pi} (C_H - i). \quad (15)$$

Here

$$C_E = \frac{\frac{\rho_m^2 - \rho_h^2}{\rho_m^2 \rho_h^2} (\text{Cos} \rho_h + \rho_h \text{Sin} \rho_h) (\text{Sin} \rho_m - \rho_m \text{Cos} \rho_m) + \rho_m \text{Cos} \rho_h \text{Cos} \rho_m + \rho_h \text{Sin} \rho_h \text{Sin} \rho_m}{\frac{\rho_m^2 - \rho_h^2}{\rho_m^2 \rho_h^2} (\text{Sin} \rho_h - \rho_h \text{Cos} \rho_h) (\text{Sin} \rho_m - \rho_m \text{Cos} \rho_m) - \rho_m \text{Sin} \rho_h \text{Cos} \rho_m + \rho_h \text{Cos} \rho_h \text{Sin} \rho_m} \quad (16)$$

and

$$C_H = \frac{-\rho_h^2 \text{Cos} \rho_h (\text{Sin} \rho_m - \rho_m \text{Cos} \rho_m) + \rho_m^2 \text{Sin} \rho_m (\text{Cos} \rho_h + \rho_h \text{Sin} \rho_h)}{\rho_h^2 \text{Sin} \rho_h (\text{Sin} \rho_m - \rho_m \text{Cos} \rho_m) - \rho_m^2 \text{Sin} \rho_m (\text{Sin} \rho_h - \rho_h \text{Cos} \rho_h)} \quad (17)$$

with  $\rho_h = k_0 n_h R$  and  $\rho_m = k_0 n_m R$ . According to Eqs. (13), (16) and (17) it follows that the power dissipated in each particle can be expressed both in term of absorption cross-sections and of incident external field

$$\begin{aligned} \mathcal{P}_i(\omega) = & -\frac{\omega}{2} \{ \varepsilon_0 \frac{n_h \omega^3}{6\pi c^3} \text{Im}[\mathbf{E}_i^{ext*} (C_E \overleftrightarrow{\alpha}_{E,i}^* \overleftrightarrow{\alpha}_{E,i}) \mathbf{E}_i^{ext}] \\ & + \mu_0 \frac{n_h^3 \omega^3}{6\pi c^3} \text{Im}[\mathbf{H}_i^{ext*} (C_H \overleftrightarrow{\alpha}_{H,i}^* \overleftrightarrow{\alpha}_{H,i}) \mathbf{H}_i^{ext}] \} \end{aligned} \quad (18)$$

To illustrate this, we show in Fig. 2 the absorption spectra at normal incidence in the visible range for TE waves of single Au and Ag spherical particles [19] dis-

persed in regular hexagonal lattices of side length  $d$  and for binary Au-Ag lattices. All lattices are immersed in a transparent material of refractive index  $n_h = 1.5$  and are maintained at a distance  $h = 100\text{nm}$  from the surface. We clearly see by comparing these absorption spectra with those of isolated particles that the resonance peaks in single particle lattices are essentially centered at the resonance frequency of free particles. However the cooperative interactions allow to increase the absorption level even in diluted lattices where the filling factor  $f$  is below 3%. This can be explained by comparing this absorption with the absorption of isolated particles (Fig. 2). It clearly appears that the absorption cross-section of

particles is strongly enhanced by the presence of neighborhood particles. The comparison of the overall absorption of nanoparticle lattices with that of simple metallic films of thickness defined from the filling factors points out importance of cooperative effects in the absorption of lattices. In binary lattices, new configurational resonances add up to the resonances of single lattices and naturally enlarge the absorption spectrum.

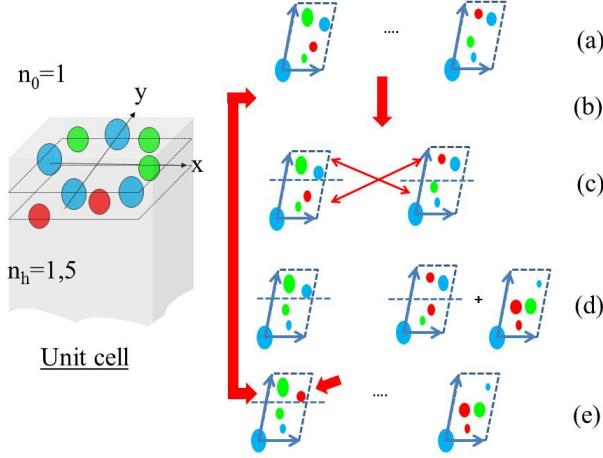


Figure 3: Evolutionary algorithm to optimize a n-ary lattice. (a) A random population of periodic lattices (a physical view of an unit cell is plotted on the left) is randomly generated. (b) The best individus based on the fitness function are selected as parents for the crossing over. (c) The next generation is created by linear crossing and completed by new individus (d) to keep the total population constant. (e) Mutations are applied on a few number of individus (typically 5%) in the current generation.

In the following, we show the strong potential of cooperative interactions mechanisms between resonators to tailor the optical properties of materials. For this purpose we present the inverse design of a broadband absorber in the visible range [6, 13–15] made with a n-ary array metallic spherical nanoparticles. A n-ary lattice is defined from a unit cell  $\mathcal{C}$  of a two dimensional paving with a certain thickness (see Fig. 3). In the unit cell of a lattice we consider a set of  $n$  vectors  $\mathbf{r}_i$  and  $n$  positive reals  $R_i$  that represent the location of particles center and the radius of particles, respectively. To avoid the particle interpenetration these vectors must satisfy to the supplemental constraint  $|\mathbf{r}_i - \mathbf{r}_j| > R_i + R_j$ . To design the n-ary lattice in order to maximize its overall absorption we have to explore the large and complex space of all possible configurations. To do that we employ a genetic algorithm (GA) [16] which is a stochastic global optimisation method that is based on natural selection rules in a similar way to the Darwin's theory of evolution. Evolutionary optimization has been yet successfully applied in numerous fields of optics [17, 18]. Basically, a GA uses an initial

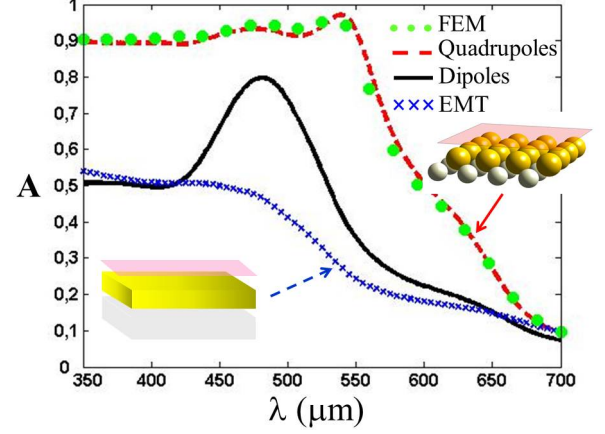


Figure 4: Light absorption spectrum at normal incidence of a binary Au-Ag lattice (blue dashed curve) optimized by GA by taking into account all multipolar interactions until the second order (quadrupoles) and of a multilayer based on Au-Ag films of thickness defined with the filling factor in nanoparticles (i.e. effective medium theory). Circles curve shows the result obtained by solving the Maxwell's equations with a finite element method.

population (Fig. 3) of typically few hundreds of structures also called individuals which are randomly generated in size and position. For each individual we calculate the fitness parameter which is here the mean absorption (for a given polarization)  $\bar{A} = (\lambda_{max} - \lambda_{min})^{-1} \int_{\lambda_{min}}^{\lambda_{max}} A(\lambda) d\lambda$  over the spectral range  $[\lambda_{min}; \lambda_{max}]$  where we want to increase the absorption. The monochromatic absorption  $A(\lambda)$  at a given wavelength is simply given by the sum of power dissipated inside the particles of the unit cell normalized by the incident flux  $\phi_{inc}(\lambda)$  on its surface  $\mathcal{A}$  that is

$$A(\lambda) = \frac{\sum_{i \in \text{Cell}} \mathcal{P}_i(\lambda)}{\mathcal{A} \phi_{inc}(\lambda)}. \quad (19)$$

The GA consists in maximizing the fitness function of structures (i.e.  $\bar{A} \rightarrow \max$ ). To do so, we select 90% of the highest fitness as future parents for the next generation of selecting process. Those parents are linearly crossed and the new 'child' generation is completed by new individual structures (randomly generated) to keep the same total number of lattices for any generation. To avoid the convergence toward local extrema, every  $m$  (typically 10) generations, we introduce also some mutations that are random perturbations with a probability of about 5% on the value of parameters we are optimizing. The results presented in Fig. 4 for superposed binary Au-Ag lattices (with the radius  $r_{Au} = 77\text{nm}$  and  $r_{Ag} = 39\text{nm}$ , the separation distances from the surface  $h_{Au} = 120\text{nm}$  and  $h_{Ag} = 242\text{nm}$ , the lattice constants  $d_{Au} = d_{Ag} = 200\text{nm}$  and the off-centring  $e_x = 56\text{nm}$  and  $e_y = 10\text{nm}$ ) exhibit a broad absorption band in the visible range. By

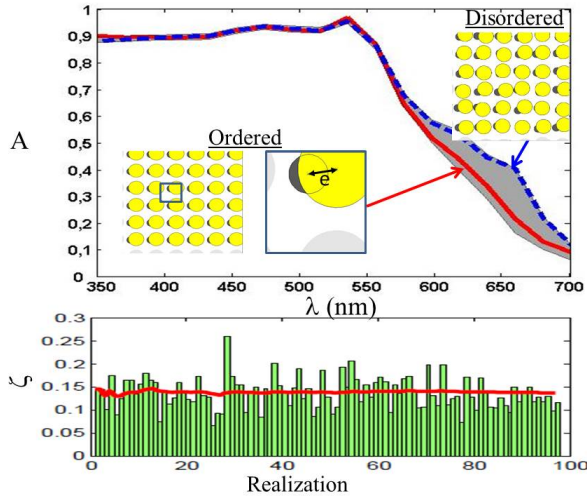


Figure 5: Impact of disorder on the light absorption spectrum at normal incidence in a binary Au-Ag lattice. The spatial location of particles is randomly perturbed by a displacement of  $20\text{nm}$ . The red curve corresponds to the spectrum (in polarization TM at normal incidence) of the optimized structure and the dotted blue curve is the spectrum of a particular random realization (results in polarization TE, not plotted here are similar). The dashed area shows the maximum and minimum values of absorption spectrum of different random realizations. The histogram shows the discrepancy with the optimal fitness for different realizations of the structure. The red line on the histogram shows the mean error with respect to the number of realizations.

taking into account the multipolar interactions until the second order (i.e. quadrupolar interactions) we see that the level of absorption becomes close to one (the comparison of these results with full electromagnetic simulations shows that the highest order multipole moments do not contribute significantly to the overall absorption).

Interestingly, the numerical simulations have shown also that the cooperative effects are not too much sensitive to the presence of disorder. In Fig. 5 we see that, by disturbing the optimal structure with a random perturbation of particles locations by a maximum displacement of  $20\text{nm}$ , the discrepancy between the optimal structure and the perturbed ones, given by the mean square error  $\zeta = [\int_{\lambda_{\min}}^{\lambda_{\max}} (A(\lambda) - A_{\text{opt}}(\lambda))^2 d\lambda]^{1/2}$ , remains small.

In conclusion, our results have demonstrated the strong potential of inverse design of cooperative interactions between optical resonators. We believe that this approach opens the way for a rational design of meta-

materials and it could find broad applications in various fields of photonics such as solar cells, quantum information systems and, according to the reciprocity principle [20] light extraction technologies.

J.-P. H. acknowledges discussions with J.J. Greffet. P. B.-A. gratefully acknowledges the support of Total news energies.

\* Electronic address: pba@institutoptique.fr

- [1] H. A. Atwater and A. Polman, *Nature Materials*, **9**, 205-213 (2010).
- [2] P. Bermel et al., *Opt. Express* **18**, A314-A334 (2010).
- [3] Ashkin A., Dziedzic J. M., Bjorkholm J. E. and Chu S., Observation of a single-beam gradient force optical trap for dielectric particles, *Opt. Lett.*, **11**, 288-290 (1986).
- [4] A. N. Poddubny, P. A. Belov and Y. S. Kivshar, *Phys. Rev. A*, **84**, 023807 (2011).
- [5] N. I. Landy, S. Sajuyigbe, J. J. Mock, D. R. Smith and W. J. Padilla, *Phys. Rev. Lett.* **100**, 207402 (2008).
- [6] K. Aydin, V. E. Ferry, R. M. Briggs and H. A. Atwater, *Nat. Comms.* **2**, 517 (2011).
- [7] S. D. Jenkins and J. Ruostekoski, *Phys. Rev. Lett.*, **111**, 147401 (2013).
- [8] V. A. Fedotovi, N. Papasimakis, E. Plum, A. Bitzer M. Walther, P. Kuo, D. P. Tsai and N. I. Zheludev, *Phys. Rev. Lett.*, **110**, 1223901 (2010).
- [9] P. Ben-Abdallah, R. Messina, S.-A. Biehs, M. Tschikin, K. Joulain, and C. Henkel, *Phys. Rev. Lett.*, **111**, 174301 (2013).
- [10] See Supplemental Material at (added by Editors).
- [11] P. Ben-Abdallah, S.-A. Biehs, and K. Joulain, *Phys. Rev. Lett.* **107**, 114301 (2011).
- [12] C. F. Bohren, D. R. Huffman, *Absorption and Scattering of Light by Small Particles* (Wiley Science, New York, 1998).
- [13] E. E. Narimanov, A. V. Kildishev, *Appl. Phys. Lett.* **95**, 041106 (2009).
- [14] A. Aubry et al., *Nano. Lett.* **10**, 2574-2579 (2010).
- [15] N. P. Sergeant, O. Pincon, M. Agrawal, P. Peumans, *Optics Express* **17**, 25, pp.22800-22812 (2009).
- [16] J. H. Holland, *Adaptation in Natural and Artificial Systems* (MIT Press/Bradford Books Edition, Cambridge, MA, 1992).
- [17] T. Feichtner, O. Selig, M. Kiunke, and B. Hecht, *Phys. Rev. Lett.* **109**, 127701 (2012).
- [18] J. Drevillon and P. Ben-Abdallah, *J. Appl. Phys.* **102**, 114305 (2007).
- [19] E. D. Palik, *Handbook of Optical Constants of Solids* (Academic Press, New York, 1998).
- [20] L. Landau, E. Lifchitz, and L. Pitaevskii, *Electromagnetism of Continuous Media* (Pergamon, Oxford, 1984).